





REGULAR PAPER

FEM-based eigenstructure recovery of a space truss with active members

L. Boni , G. Mengali , A.A. Quarta  and M. Bassetto 

Department of Civil and Industrial Engineering, University of Pisa, 56122 Pisa, Italy

Corresponding author: A.A. Quarta; Email: a.quarta@ing.unipi.it

Received: 10 October 2023; Revised: 19 February 2024; Accepted: 12 March 2024

Keywords: large flexible structures; damage assessment; finite element method; system identification; piezoelectric sensor/actuators; structural behavior control

Abstract

Large truss structures have many potential applications in space, such as antennas, telescopes and space solar power plants. In this scenario, a natural concern is the susceptibility of these lightweight structures to be damaged during their operational life, due to impacts, transient thermal states and fatigue phenomena. The inclusion of active elements, equipped with sensor/actuator systems capable of modulating their shape and strength, makes it possible to transform the truss into a smart structure capable of remedying the damage, once it is detected. In this paper, a procedure is described that is capable of restoring at least the basic functionality of a composite truss for space applications, starting with the observation that damage has occurred, regardless of its specific location. The system eigenstructure is used as a benchmark for damage detection, as well as a target characteristic for the subsequent restoration activity. The observer/Kalman filter identification algorithm (OKID), in cascade with the eigensystem realization algorithm (ERA), is adopted to reconstruct, from sensor recordings, the dynamic response of the truss in terms of system state-space representation and eigen-characteristics. Finally, a static output feedback control is developed to recover the low-frequency dynamic behaviour of the truss. The entire procedure is tested using finite element analysis. All activities are coordinated in an innovative procedure that, within a unique Python language code, automatically generates finite element (FE) models, launches finite element analysis (FEA), extracts output data, implements OKID-ERA, processes the control law and applies it to the final FE simulation.

Nomenclature

A	state matrix
B	input matrix
C	output matrix
D	feedforward matrix
I	identity matrix
K	constant feedback gain matrix
ℓ	$n - r > 0$
L_i	auxiliary matrix
m	dimension of \mathbf{u}
n	dimension of \mathbf{x}
r	dimension of \mathbf{y}
t	time
\mathbf{u}	input (or control) vector
U	auxiliary matrix
V	auxiliary matrix
\mathbf{x}	state vector
\mathbf{y}	output vector
\mathbf{z}	transformed state vector

Greek Symbol

λ_i	generic eigenvalue
\mathbf{v}_i	generic eigenvector

Subscripts

a	augmented
Cl	closed loop
ℓ	of dimension equal to ℓ
r	of dimension equal to r

Superscripts

a	achievable
d	desired
\dagger	Moore-Penrose inverse
\sim	transformed
\cdot	time derivative

1.0 Introduction

The already-widespread use of large flexible structures in space applications is set to grow further in the future due to the advantageous combination of low weight and high packing efficiency they offer. The introduction of carbon fibre composite materials, with their high stiffness and low thermal expansion, has made their use in the space environment even more attractive. In recent years, thanks to advances in smart materials and robotic manufacturing techniques, interest has extended to deployment procedures [1] and to the construction and assembly of trusses directly in space [2]. The increased time in space also increases the probability that various combinations of events, both mechanical and thermal, will damage these very slender structures, compromising their proper functioning. The problem of detecting damage and maintaining the performance of structural systems is of general interest, but becomes of primary importance for space components due to the high cost of missions. For this reason, the problem of health monitoring and maintenance procedures has received a great deal of interest since the 1990s, both in the field of system identification and in that of control design, giving rise to a series of studies related to this problem. Some of these works relate the change in the physical properties of the system to a change in the stiffness and mass matrices [3–5] or to an alteration in the curvature of the mode shape induced by damage [6]. Other authors focus their attention on the variation of state-space representation parameters [7, 8]. The use of neural networks has also been emphasised in the past [9, 10] and continues to be of interest [11]. More recent work considers machine learning as a powerful tool for ‘novelty detection’ [12–14]. Another approach that has been widely developed in recent years involves the use of probabilistic methodologies to determine structural damage and identify the damaged structure taking into account model uncertainties [15–17]. In particular, the use of Bayesian system identification has received considerable interest to obtain reliable structural models based on the dynamic response of the system [18–20]. The most recent trend is to exploit the close link between machine learning and system identification [21].

In the specific case of a truss, the problem was addressed by taking advantage of the discrete nature of skeleton structures, which typically suffer damage limited to a few elements, with the rest still intact. The current level of technology has made active members, equipped with complex systems of sensors, processors and actuators, feasible tools for both health monitoring and maintenance activities [22]. The crucial aspect of this strategy remains the difficulty of remotely and promptly detecting the onset of damage and, even more so, determining its exact location and extent. In fact, in the case where alterations in vibrational response are the main cause of loss of function in space applications, efforts should

be directed at recovering the low-frequency dynamic response after damage detection, regardless of its specific allocation. In this scenario, this paper discusses a procedure to ensure that the main operational requirements of a composite truss for use in space are again met through the recovery of vibrational behaviour under damage-free conditions. The control, as conceived in this work, aims to allow the system to maintain its operational functions, possibly with degraded capabilities, until a repair operation is possible. For the sake of generality, approaches to restoring space mission requirements depend strictly on the specific objective and may be different in nature. For example, if accurate pointing of an on-board mounted antenna is paramount, it may be necessary to constrain maximum displacements and/or rotations between specific points on the structure. In this paper, the focus is on another fundamental aspect common to many missions, namely, avoiding interference between structural and instrumentation modes, so keeping the structure's natural frequencies within prescribed limits is critical. The eigenstructure of the system is used as a comparison term to detect the damage and as a target property for the recovery activity. In fact, a control law is developed to reestablish the pristine values of the first eigenvalues and eigenvectors. The OKID procedure, in cascade with the ERA, is adopted to reconstruct the dynamic response of the truss from measurements taken by sensors, placed at strategic locations (more details will be given in Section 3). Once the state-space representation and eigen-characteristics of both health and damaged structure are available, a static output feedback control is established to recover the low-frequency dynamic behaviour. A FEA is used to test the effectiveness of the approach by developing numerical models of intact and damaged structures, with damage introduced in the form of passive rod removal. Since the exact location of the damage is not known a priori, both the number and the arrangement of the removed rods are free parameters, with the only constraint being to ensure the controllability of the system. The finite element analysis provides the input data for the OKID-ERA algorithm, as well as to provide reference eigenstructure and vibrational response to external loads, to be compared with those predicted by the identified systems. Finally, the control law is implemented in the FE model, in the form of displacements imposed on the active members, to add information about its effects on the stress-strain field of the entire truss. All activities are successfully coordinated by developing an innovative procedure that, within a single script in Python language, automatically generates the FE models, launches the FEAs, extracts the output data, implements OKID-ERA, processes the control law and applies it to the final FE simulation.

The paper is organised as follows. Section 2 outlines the problem and describes the general architecture of the procedure used. System identification, control law and FEA are discussed in Sections 3, 4 and 5, respectively. Section 6 presents some numerical examples to demonstrate the effectiveness of the proposed procedure and, finally, Section 7 draws our conclusions.

2.0 Problem statement and procedure architecture

A flat truss structure, entirely made of high-stiffness composite material for typical aerospace use, is considered as a test sample and is shown in Fig. 1. Three of the 46 rods are active and equipped with sensors (to monitor the outputs) and actuators (to apply the input forces). Although an in-depth study of the properties of the sensor/actuator system is beyond the scope of this paper, piezoelectric elements of '1–3 rod composite' [23] are considered optimal for the present purpose. Indeed, like all piezoelectric devices [24], they can act simultaneously as sensors and actuators due to their ability to translate mechanical force into electrical energy and vice versa. In addition, their constituent material is a high-stiffness composite, with properties very similar to those of passive rods, so as to authorise their full assimilation with the remaining members when in the passive phase. Actuators, strategically located, are supposed to excite only the structural modes of interest, while sensors are supposed to measure the corresponding modes.

An external random excitation is considered to simulate the action of a thruster, in the hypothesis of measuring its force by sensors.

The various phases of the procedure are accomplished by means of a combined and integrated use of FEM, Python scripting and Fortran programming. Indeed, the Python language is used to develop

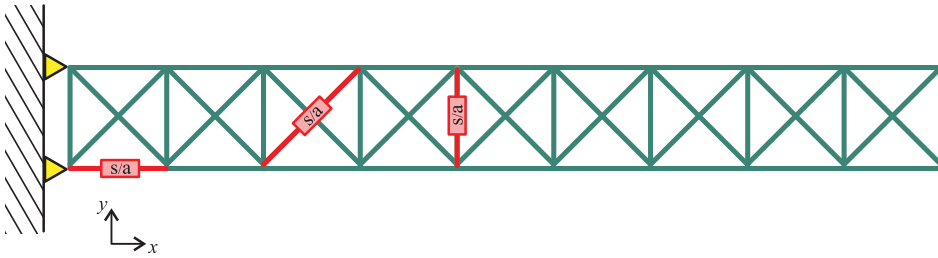


Figure 1. Schematic view of a space truss with three piezoelectric sensors/actuators.

a unique code, divided into several scripts, both to perform pre- and post-processing tasks within the Abaqus 2022 FE software and to implement system identification and feedback control algorithms; see the block diagram in Fig. 2. In addition, a dedicated subroutine was created in Fortran language to process the control law in FEA. This specific approach is made possible by the well-established FE modeling technique through Python scripting [25], the communication between FE processing and Fortran subroutines [26], the use of specific Python modules for scientific [27] and array [28] calculation, and for control system development [29–31].

Two different versions of Python are used, namely the older Python 2.7, which is the only one supported by the Abaqus software, and the newer Python 3.11, due to the integration of its libraries with control system techniques. The use of Pickle files enables total communication between scripts written in different Python versions. Indeed, a Pickle file can serialises Python object structures, by converting an object in memory into a stream of bytes to be stored as a binary file on disk. Once re-loaded into a Python program, this binary file can be de-serialised into a Python object.

3.0 System identification

Over the years, many system identification techniques have been developed for space structure applications to cope with their extremely low damping [32]. In this context, Markov parameters [33] arise in a realisation theory that finds a state-space representation of a linear time-invariant system from its pulse response. The disadvantage of solving the Markov parameters of the system directly in the time domain from the input and output data is the need to invert an input matrix that becomes very large for slightly damped systems. In this respect, one possible solution to this problem is to obtain, again from input-output data of the system to be identified, the Markov parameters of an asymptotically stable observer. This method, chosen in the present work, is called the OKID [34] and consists of a procedure in which the state-space model and the corresponding observer are determined simultaneously.

Using a Kalman filter as an observer overcomes the problem of signals disturbed by noise. In the matrix formulation developed by Phan et al. [34], the Markov parameters of the system can be uniquely obtained from those of the observer/Kalman filter. Once observer and system Markov parameters are determined, the ERA [35] is used to realize the state-space model. Thus, the method referred to as OKID/ERA provides an identification of the undamaged structure (before) and of the damaged structure (after) with a state-space model in the following form

$$\begin{cases} \dot{\mathbf{x}} = \mathbf{A} \mathbf{x} + \mathbf{B} \mathbf{u} \\ \mathbf{y} = \mathbf{C} \mathbf{x} + \mathbf{D} \mathbf{u} \end{cases} \quad (1)$$

where $\mathbf{x} \in \mathbb{R}^n$ denotes the system state, $\mathbf{u} \in \mathbb{R}^m$ is the input (or control) variable, and $\mathbf{y} \in \mathbb{R}^r$ is the output variable. Note that \mathbf{x} , \mathbf{u} , and \mathbf{y} are all functions of time t . Moreover, without loss of generality, it is assumed that $m < r < n$, that is, the number of measured outputs exceeds the number of inputs. The physical nature of the identified state is not known a priori because OKID algorithm selects only the set

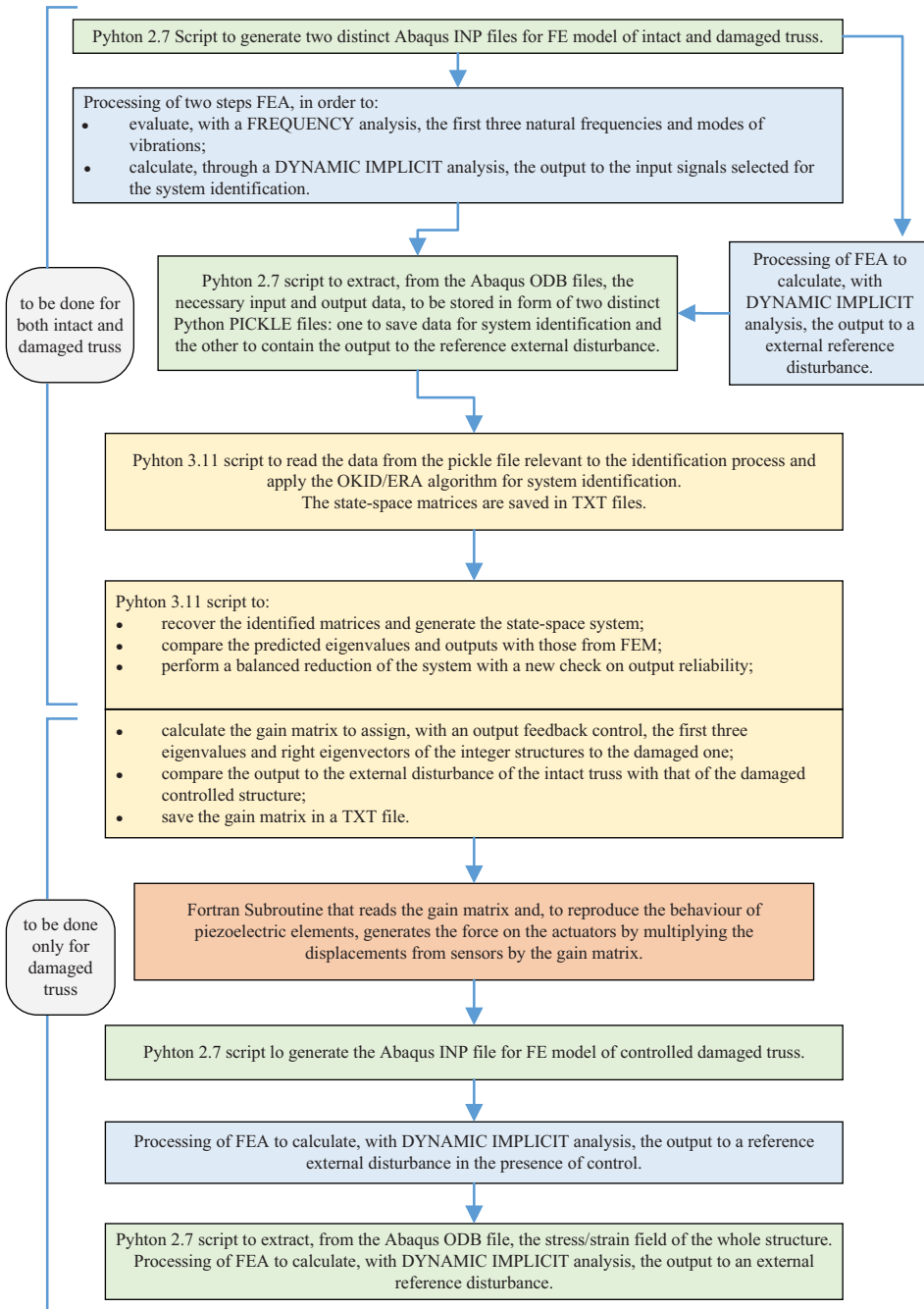


Figure 2. Block diagram of the proposed procedure.

of matrices $\{A, B, C, D\}$ that best correlate input with output data. A state transformation can anyway help in giving a clear meaning to \mathbf{x} . In particular, if the system order is equal to the number of outputs (i.e. if $r = n$), the matrix C is square and can be inverted. Thus, by introducing the transformation

$$\mathbf{z} = \mathbf{C} \mathbf{x} \tag{2}$$

the following state-space system is obtained

$$\begin{cases} \dot{\mathbf{z}} = \tilde{\mathbf{A}}\mathbf{z} + \tilde{\mathbf{B}}\mathbf{u} \\ \mathbf{y} = \tilde{\mathbf{C}}\mathbf{z} \end{cases} \quad (3)$$

where

$$\tilde{\mathbf{A}} = \mathbf{C}\mathbf{A}\mathbf{C}^{-1}, \quad \tilde{\mathbf{B}} = \mathbf{C}\mathbf{B}, \quad \tilde{\mathbf{C}} = \mathbf{I} \quad (4)$$

According to this transformation, the state variables acquire a clear physical meaning: system outputs and state variables are all coincident with nodal displacements.

However, in the case where the order of the system is greater than that of the measured outputs ($n > r$), it turns out that \mathbf{C} is rectangular, thus not invertible. To proceed as above, firstly the state vector is partitioned as

$$\mathbf{x} = \begin{bmatrix} \mathbf{x}_r \\ \mathbf{x}_\ell \end{bmatrix}$$

with $\mathbf{x}_r \in \mathbb{R}^r$, $\mathbf{x}_\ell \in \mathbb{R}^\ell$ and $\ell = n - r$ in such a way that

$$\mathbf{y} = \begin{bmatrix} \mathbf{C}_1 & \mathbf{C}_2 \end{bmatrix} \begin{bmatrix} \mathbf{x}_r \\ \mathbf{x}_\ell \end{bmatrix}$$

Then, an augmented output vector is introduced as

$$\mathbf{y}_a = \begin{bmatrix} \mathbf{y} \\ \mathbf{x}_\ell \end{bmatrix} = \mathbf{C}_a \begin{bmatrix} \mathbf{x}_r \\ \mathbf{x}_\ell \end{bmatrix} \quad (5)$$

where

$$\mathbf{C}_a = \begin{bmatrix} \mathbf{C}_1 & \mathbf{C}_2 \\ \mathbf{0} & \mathbf{I}_\ell \end{bmatrix} \quad (6)$$

and $\mathbf{I}_\ell \in \mathbb{R}^{\ell \times \ell}$ is the identity matrix. After this artificial extension of the outputs, the state-space model can be transformed as follows:

$$\dot{\mathbf{z}} = \mathbf{C}_a \mathbf{x} \quad (7)$$

which now plays the role of Equation (2). Following the above procedure, the system representation becomes

$$\dot{\mathbf{z}} = \tilde{\mathbf{A}}\mathbf{z} + \tilde{\mathbf{B}}\mathbf{u} \quad (8)$$

$$\mathbf{y} = \tilde{\mathbf{C}}\mathbf{z} \quad (9)$$

where

$$\tilde{\mathbf{A}} = \mathbf{C}_a \mathbf{A} \mathbf{C}_a^{-1} \quad (10)$$

$$\tilde{\mathbf{B}} = \mathbf{C}_a \mathbf{B} \quad (11)$$

$$\tilde{\mathbf{C}} = \begin{bmatrix} \mathbf{I}_r & \mathbf{0} \end{bmatrix} \quad (12)$$

The transformation of the state variables of Equation (7) provides clear physical meaning to the identified state space systems because the same type of transformation gives identical meaning to the state variables of the undamaged and damaged structure models, allowing them to be compared. Because of this comparability, system identification techniques enable health monitoring of the structure throughout its life. This can be done by applying independent, time-varying forces through the piezoelectric actuators as well as a disturbance external to the structure. The first identification, in undamaged conditions, represents a reference for those subsequently done: changes in the truss low frequency modes may indicate that damages have crept in the structure and would lead to its replace or refurbish.

4.0 Control law

Once the presence of damage is detected, the problem is how to restore, at least partially, the dynamic behaviour of the structure. In this work, the damaged truss is forced to behave like the intact one by means of a static output feedback controller. Moreover, due to the state transformation in Equation (12), the output feedback behaves as a state feedback designed to match the identifiable eigenvalues and corresponding right eigenvectors of the intact with those of the damaged structure. Accordingly, the control law is in the form

$$\mathbf{u} = K \mathbf{y} \quad (13)$$

where K is the constant feedback gain matrix and the state matrix in closed loop becomes

$$\tilde{A}_{cl} = \tilde{A} + \tilde{B} K \tilde{C} \quad (14)$$

As shown by Srinathkumar [36], $\max(m, r)$ closed loop eigenvalues can be arbitrarily assigned with $\min(m, r)$ components of the corresponding right eigenvectors, provided the system is controllable and observable. The gain matrix can be calculated according to the method developed by Andry et al. [37], which accounts for the concept of achievable eigenvectors. Indeed, as explained in Ref. (36), it is not possible to completely assign the right eigenvectors of the controlled system, but it is possible to guarantee that the desired eigenvectors are “best” approximated in a least square sense.

According to this procedure, if λ_i is a generic eigenvalue and \mathbf{v}_i^d is the desired right eigenvector, the corresponding achievable eigenvector is

$$\mathbf{v}_i^a = L_i L_i^\dagger \mathbf{v}_i^d \quad (15)$$

where

$$L_i = (\lambda_i I - \tilde{A})^{-1} \tilde{B} \quad (16)$$

and L_i^\dagger is the Moore-Penrose inverse of L_i . The final expression of the gain matrix discussed in Ref. (37) is obtained only for a special state transformation addressed to simplify the B matrix structure. In this work, the original procedure has been modified accordingly to be compliant with the state transformation in Equation (3). The obtained expression of the feedback matrix is

$$K = U (\tilde{C} V)^{-1} = \tilde{B}^{-1} U (V)^{-1} \quad (17)$$

where the columns of matrix V are the achievable eigenvectors and the columns of matrix U are related to the achievable eigenvalues and eigenvectors. Note that, as pointed out in Ref. (37), when the number of poles to be placed is smaller than the dimension of the state matrix the feedback control can adversely affect some of the unconstrained eigenvalues such that system instability can result. In the problem at hand, this phenomenon has been avoided by making $r = n$ with a balanced reduction of the identified systems.

5.0 Finite element models

The FE model of the nine-bay truss shown in Fig. 1 is executed entirely by Python scripting. The truss structure is made of 46 graphite/epoxy rods with hollow circular cross section of mean radius 340 mm and thickness 2 mm. The length of each non-diagonal element is 1.5 m. The material is assumed to be homogeneous with density 1700 kg/m³ and isotropic, according to the one-dimensional nature of rod elements, with Young's modulus equal to 90 GPa, coincident with the E11 value of the actual composite material. No type of damping is assigned to this material. The 2-node linear 2-D truss elements of type T2D2 are used for the rods, while axial connectors elements are adopted to model the piezoelectric sensor/actuators. Each connector, which has the same elastic stiffness as the rods, behaves as a generic truss element if no axial displacements or forces are externally imposed to promote its function as an actuator. The structure is clamped at the left end, while an external excitation normal to the longitudinal axis of the truss is applied to the right upper end node. A Gaussian white noise is added to the excitation

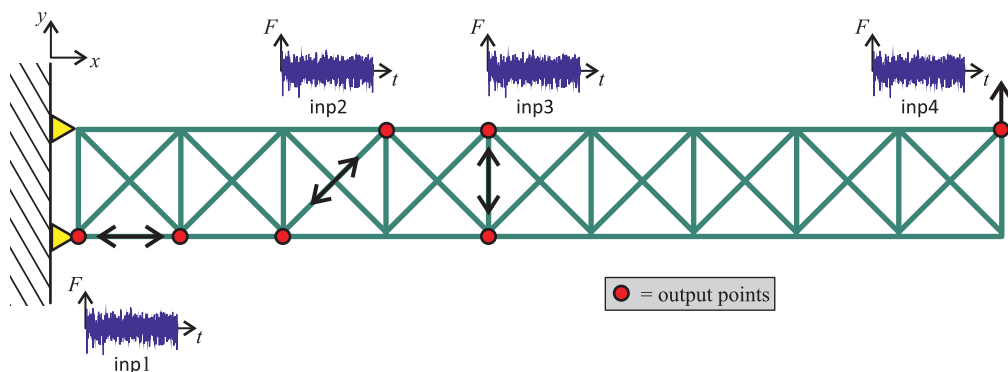


Figure 3. Scheme of the inputs for system identification.

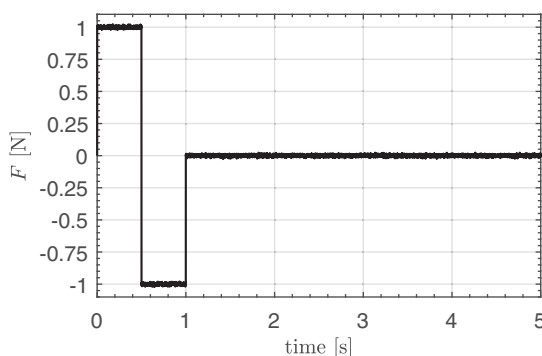


Figure 4. Time history of the external force.

to simulate the presence of an external disturbance. Three actuators are supposed to be located in the horizontal, vertical and diagonal direction as shown in Fig. 1. The location of the actuators is based upon simplified controllability considerations (singular values analysis).

The FE model of the undamaged truss originates three different types of analysis: (i) to calculate the lowest three natural frequencies and modes of vibrations of the structure; (ii) to enable system identification; (iii) and to record the response to external excitation. The first two analyses are grouped and cascaded as a frequency step followed by one of dynamic implicit type. In the last analysis, a single dynamic implicit step is processed. In each case, the simulation lasts 5 seconds and is based on the implicit operator defined by Hilber et al. [38] for the temporal integration of the dynamic problem. The set of input data used to identify the system is shown in Fig. 3: axial forces are applied to the actuators and a transversal force at the upper left node of the truss, all following a time history based on white noise. The white noise amplitude is generated with zero mean value, unitary standard deviation, and 2×10^3 frequency. The vertical component of displacement and velocity are recorded at the ends of the actuators and at the upper right node as output data, as shown in Fig. 3. The system to be identified has 4 inputs and 14 outputs. The last analysis is addressed to record the vertical displacement of the left upper node when the external transversal force with double-step amplitude shown in Fig. 4 acts on it.

The FE model of the damaged structure is obtained by simply removing some passive members: in the example shown in Fig. 5, two horizontal rods are removed from the top of the truss. All FEAs performed on the undamaged truss are repeated for the damaged structure. A final analysis is then added to simulate the control law developed to restore the dynamic behaviour of the truss. This analysis exploits the possibility of defining a load history through an external subroutine written in Fortran.

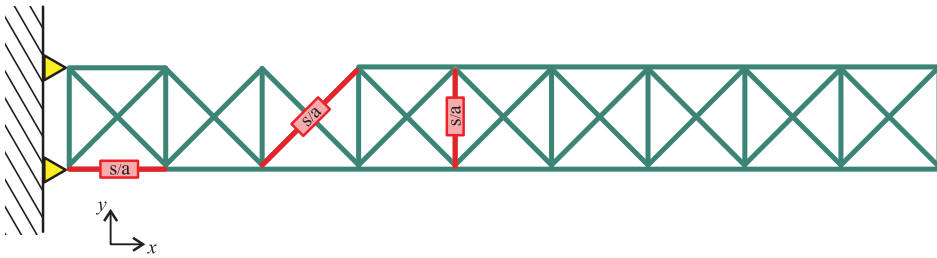


Figure 5. Introduction of damage as member removal.

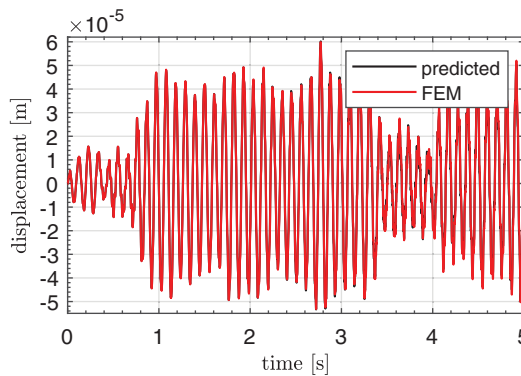


Figure 6. Comparison between FEM and predicted outputs for undamaged truss with white noise input.

In addition, the Abaqus software allows sensors to be placed at strategic nodal points that can transmit the desired output variables to the subroutine at each time increment. Once the control gain matrix is defined according to the procedure described in Section 4, its coefficients are copied into the subroutine and used to define the loads on the actuators as a linear combination of their end displacements, continuously updated by the sensors. In the latter analysis, a dynamic implicit step is implemented, in which the external load and the control forces act simultaneously.

6.0 Numerical results

6.1 System identification

The Python script that implements the OKID/ERA algorithm, according to the procedure described in Section 3, provides the four matrices $\{A, B, C, D\}$ necessary to define the discrete space-state model of the truss. The identified 14th-order model with a time interval of 0.005 seconds is assembled and then transformed into continuous form in a dedicated Python script. The response of the system is simulated to both input loads used for its identification and to the external double step force. All these results are obtained for both undamaged and damaged structure. In view of the control strategy development, for the damaged truss, a balanced reduction is applied to the system, in order to decrease its order from 14 to 6, which is double the number of complex poles to be allocated.

The proposed methodology depends heavily on the effectiveness of the OKID/ERA algorithm in identifying a dynamic system with realistic behaviour. Because of the importance of an experimental reference, the results provided by FEA are used, in this paper, as reference values. As an example, for the undamaged structure, Fig. 6 shows the displacement in vertical direction of the upper right node of the truss in case of white noise input used for identification. A perfect superposition between the two data sets is clearly visible.

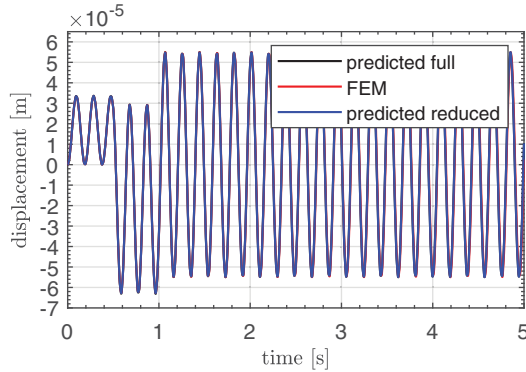


Figure 7. Comparison between FEM and predicted outputs for damaged truss with external double step force.

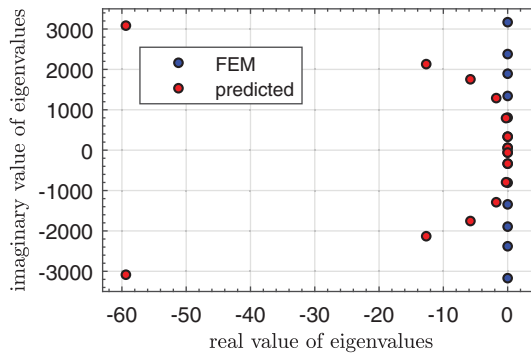


Figure 8. Comparison between FEM and predicted eigenvalues for undamaged truss.

For the damaged truss, the FE results are compared with the responses predicted by both the full and reduced order system. As an example, Fig. 7 shows the displacement in vertical direction of the upper left node of the truss for the case of external double step force. The graph in figure highlights the excellent ability of the identified system, even in its reduced form, to capture the structural response.

In Fig. 8, the eigenvalues extracted from FEAs are compared with the 14 of the identified systems for the undamaged truss case. The frequency step implemented in Abaqus allows to calculate the eigenvalues of the symmetrised system, that is, neglecting damping or any source of asymmetry in the stiffness matrix. The symmetrised system has real squared eigenvalues λ^2 and real eigenvectors only: if the stiffness matrix is positive semidefinite there are only pairs of conjugate imaginary eigenvalues $\pm\lambda i$, where λ is the circular frequency [39]. The eigenvalues identified by FEAs are accordingly aligned on the imaginary axis, symmetrically distributed with respect to the real axis. In contrast, the eigenvalues of the identified system depend on the input/output data of the dynamic implicit step and can capture any source of damping.

Despite the absence of intrinsic material damping, the operator adopted to integrate the dynamic equations is characterised by user-defined numerical damping, which varies from a minimum in transient fidelity analyses to a maximum in steady-state ones. The nature of artificial numerical damping is to damp out unwanted high-frequency modes to reduce the simulation time up to steady state conditions. When performing transient fidelity analysis, as in the present study, lower frequencies are not altered by artificial damping, while the higher the frequencies, the more they are damped. This phenomenon is evident in Fig. 8, where the predicted poles lie on a pseudo-ellipse arc tangent to the imaginary axis:

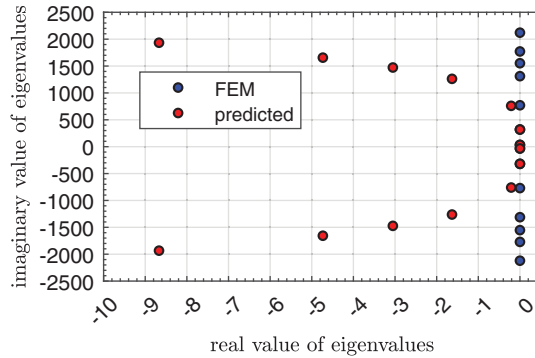


Figure 9. Comparison between FEM and predicted eigenvalues for damaged truss.

the three lowest frequencies of FEAs, related to the poles highlighted in red, are totally coincident with the predicted ones. In Fig. 9, a similar comparison between the predicted and FE eigenvalues is made for the undamaged truss case. The predicted poles, compared with the previous case, are slightly more damped, consistently with the dynamic behaviour of artificial damping, which varies according to the convergence performance of the specific FE model.

6.2 Control strategy

In the control strategy outlined in Section 4, the application of an output-feedback control law was simulated in such a way that the first three complex eigenvalues and the components of the right eigenvectors of the healthy structure can be assigned to the damaged structure to restore, at least in part, the dynamic behaviour of the truss.

In Fig. 10, it is possible to directly compare the first eigenvalues of the two systems and observe the effect of the controller. As is evident from the figure, only the imaginary part of the poles was considered in the control strategy. The vertical displacement of the upper right node due to the double step force is shown in Fig. 11 for the undamaged, damaged and controlled structure. From the figure, a substantial overlap between the structural response of the undamaged truss and the controlled truss can be seen: the controller, designed to simply recover the healthy eigenstructure, also shows good trajectory tracking capability in the presence of an external force.

The effects of control on the structure is finally studied by simulating it in a dedicated FEA, as explained in Section 5. The overlay plot tool, available in Abaqus, allows to superimpose the deformation of the whole truss in undamaged and damaged-controlled conditions. In particular, Fig. 12 shows the displacement field at an instant of maximum vibration amplitude. From this figure, it is possible to detect the substantial effectiveness of the controller in recovering the healthy structural behaviour along the whole truss axis and not only at the point of external force application.

Another important aspect is the possibility of designing the controller not only to recover but also to improve the dynamic response of the structure. In fact, it is possible to add damping to the vibrations simply by placing poles with negative real part. For example, looking at Fig. 13, the control restores frequencies to their original values and, at the same time, adds damping by placing poles with negative real part of 0.25.

7.0 Conclusions

The procedure adopted for damage detection and eigenstructure recovering of a composite truss for space application equipped with active members has shown great promise. The salient aspects are the

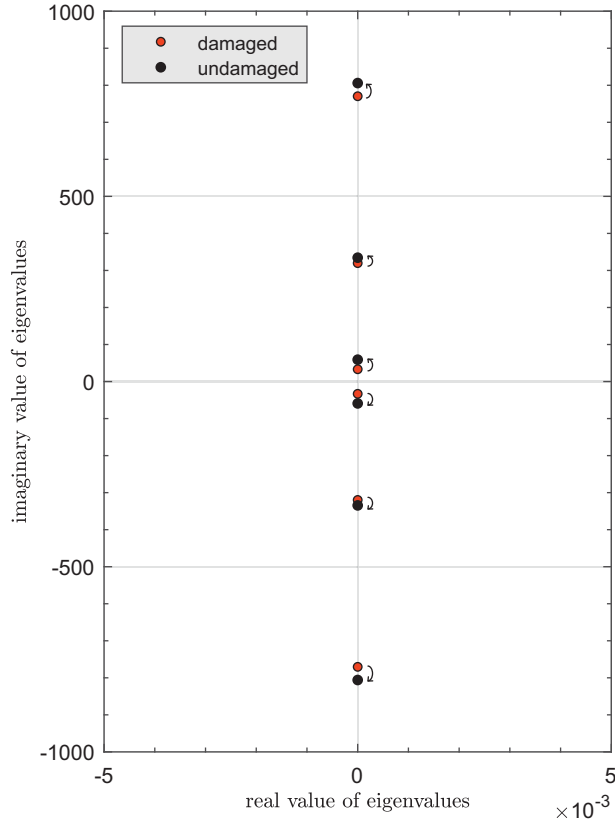


Figure 10. Comparison between eigenvalues of undamaged and damaged truss.

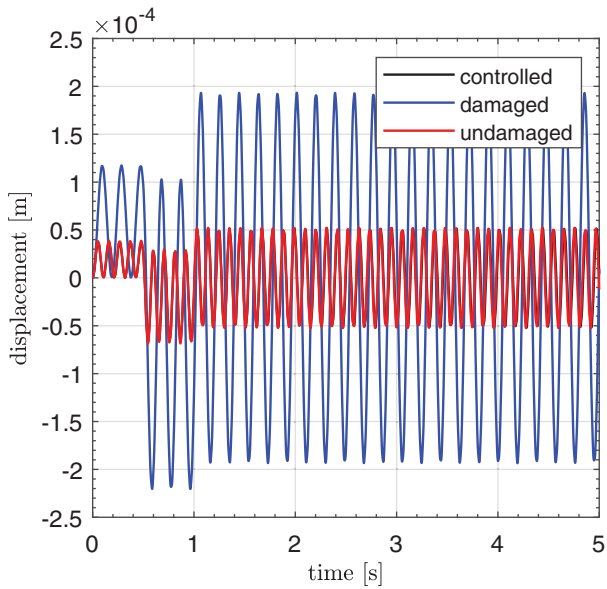


Figure 11. Comparison between structural response of undamaged, damaged and controlled truss.

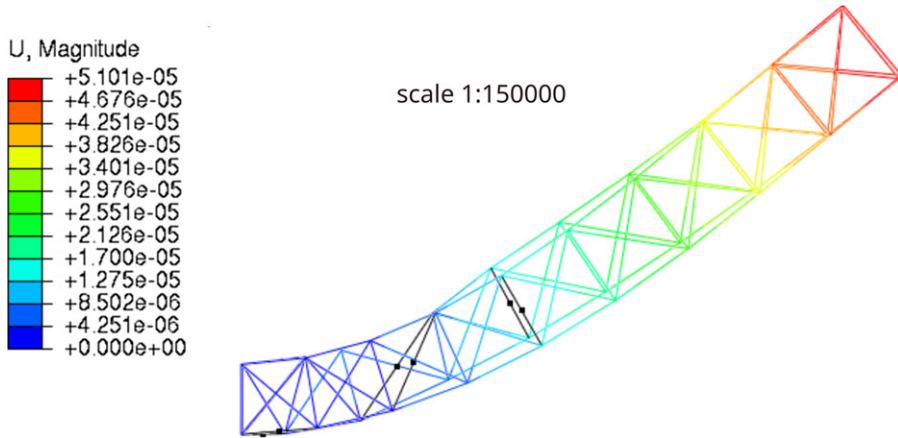


Figure 12. Overlay plots of truss deformations in undamaged and damaged-controlled conditions.

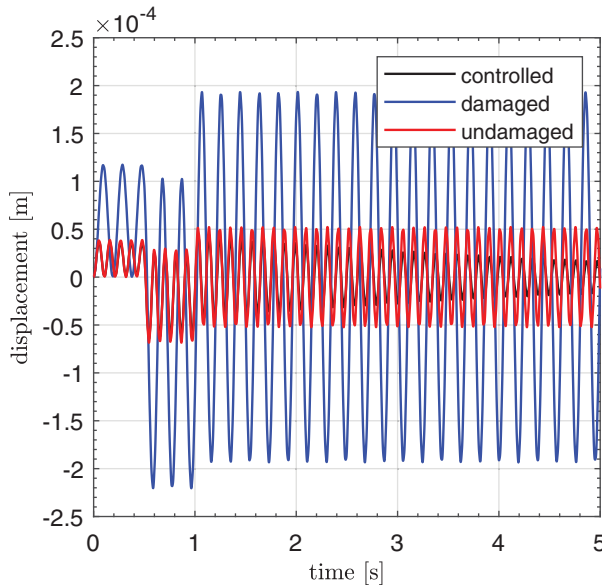


Figure 13. Comparison between structural response of undamaged, damaged and controlled truss with added damping.

possibility of ignoring the exact location of damage, the total automation of the procedure, the versatility in adding damping, and the final verification of the whole structure. The application of the proposed methodology relies on the availability of experimental sensor records, but FEM is a valuable tool for setting up and testing the various steps. In addition, the combined use of FEM and programming languages such as Python and Fortran lends robustness to the control strategy, representing an essential tool to verify the stress/strain state of the structure at each material point. In a scenario of increasing use of large composite trusses in expensive space missions, this work is likely to contribute to improving the management and exploitation of these lightweight structures.

Acknowledgements. The authors would like to thank Andrea Pieracci for his advice that inspired this work.

References

- [1] Puig, L., Barton, A. and Rando, N. A review on large deployable structures for astrophysics missions, *Acta Astronaut.*, 2010, **67**, (1), pp 12–26. <https://doi.org/10.1016/j.actaastro.2010.02.021>
- [2] Cheng, Z., Hou, X., Zhang, X., Zhou, L., Guo, J. and Song, C. In-orbit assembly mission for the space solar power station, *Acta Astronaut.*, 2016, **129**, pp 299–308. <https://doi.org/10.1016/j.actaastro.2016.08.019>
- [3] Alvin, F.K., Peterson, D.L., and Park, C.K. Method for determining minimum-order mass and stiffness matrices from modal test data, *AIAA J.*, 1995, **33** (1), pp 128–135. <https://doi.org/10.2514/3.12342>
- [4] Peterson, L.D., Alvin, K.F., Doebling, S.W. and Park, K.C. Damage detection using experimentally measured mass and stiffness matrices, In *AIAA/ASME/ASCE/AHS/ASC 34th Structures, Structural Dynamics, and Materials Conference*, 19–22 April, La Jolla, USA, 1993. AIAA. <https://doi.org/10.2514/6.1993-1482>
- [5] Zimmerman, D.C. and Simmermacher, T. Model correlation using multiple static load and vibration tests, *AIAA J.*, 1995, **33**, (11), pp 2182–2188. <https://doi.org/10.2514/3.12813>
- [6] Pandey, A.K., Biswas, M. and Samman, M.M. Damage detection from changes in curvature mode shapes. *J. Sound Vibr.*, 1991, **145**, (2), pp 321–332. [https://doi.org/10.1016/0022-460X\(91\)90595-B](https://doi.org/10.1016/0022-460X(91)90595-B)
- [7] Alvin, K.F. and Park, K.C. Second-order structural identification procedure via state-space-based system identification, *AIAA J.*, 1994, **32**, (2), pp 397–406. <https://doi.org/10.2514/3.11997>
- [8] Lew, J.-S. Using transfer function parameter changes for damage detection of structures, *AIAA J.*, 1995, **33**, (11), pp 2189–2193. <https://doi.org/10.2514/3.12965>
- [9] Povich, C. and Lim, T. An artificial neural network approach to structural damage detection using frequency response functions, In *Adaptive Structures Forum*, 21–22 April, Hilton Head, USA, 1994. <https://doi.org/10.2514/6.1994-1751>
- [10] Tsou, P. and Herman Shen, M.-H. Structural damage detection and identification using neural networks, *AIAA J.*, 1994, **32**, (1), pp 176–183. <https://doi.org/10.2514/3.11964>
- [11] Abdeljaber, O., Avci, O., Kiranyaz, S., Gabbouj, M. and Inman, D.J. Real-time vibration-based structural damage detection using one-dimensional convolutional neural networks, *J. Sound Vibr.*, 2017, **388**, pp 154–170. <https://doi.org/10.1016/j.jsv.2016.10.043>
- [12] Farrar, C.R. and Worden, K. *Structural Health Monitoring: A Machine Learning Perspective*. John Wiley & Sons, Chichester, UK, 2013.
- [13] Ozdagli, A.I. and Koutsoukos, X. Machine learning based novelty detection using modal analysis, *Comput.-Aided Civil Infrastruct. Eng.*, 2019, **34**, (12), pp 1119–1140. <https://doi.org/10.1111/mice.12511>
- [14] Parisi, F., Mangini, A.M., Fanti, M.P. and Adam, J.M. Automated location of steel truss bridge damage using machine learning and raw strain sensor data, *Automat. Construct.*, 2022, **138**, pp 1–13. Article no. 104249. <https://doi.org/10.1016/j.autcon.2022.104249>
- [15] Entezami, A., Sarmadi, H. and De Michele, C. Probabilistic damage localization by empirical data analysis and symmetric information measure, *Measurement*, 2022, **198**, pp 1–19. Article no. 111359. <https://doi.org/10.1016/j.measurement.2022.111359>
- [16] Mengali, G. and Pieracci, A. Probabilistic approach for integrated structural control design, *AIAA J.*, 2000, **38**, (9), pp 1767–1769. <https://doi.org/10.2514/2.1170>
- [17] Yan, W.-J., Chronopoulos, D., Yuen, K.-V. and Zhu, Y.-C. Structural anomaly detection based on probabilistic distance measures of transmissibility function and statistical threshold selection scheme, *Mech. Syst. Sig. Process.*, 2022, **162**, pp 1–22. Article no. 108009. <https://doi.org/10.1016/j.ymsp.2021.108009>
- [18] Huang, Y., Beck, J.L. and Li, H. Bayesian system identification based on hierarchical sparse Bayesian learning and Gibbs sampling with application to structural damage assessment, *Comput. Methods Appl. Mech. Eng.*, 2017a, **318**, pp 382–411. <https://doi.org/10.1016/j.cma.2017.01.030>
- [19] Huang, Y., Beck, J.L. and Li, H. Hierarchical sparse bayesian learning for structural damage detection: theory, computation and application, *Struct. Saf.*, 2017b, **64**, pp 37–53. <https://doi.org/10.1016/j.strusafe.2016.09.001>
- [20] Huang, Y., Shao, C., Wu, B., Beck, J.L. and Li, H. State-of-the-art review on bayesian inference in structural system identification and damage assessment, *Adv. Struct. Eng.*, 2019, **22**, (6), pp 1329–1351. <https://doi.org/10.1177/1369433218811540>
- [21] Ljung, L., Andersson, C., Tiels, K. and Schön, T.B. Deep learning and system identification, *IFAC-PapersOnLine*, 2020, **53** (2), pp 1175–1181. <https://doi.org/10.1016/j.ifacol.2020.12.1329>
- [22] Toklu, Y.C. and Arditi, D. Smart trusses for space applications. In *Engineering for Extreme Environments*, October 27–29, 2014, St. Louis, Missouri, USA, 2014.
- [23] Chee, C.Y.K., Tong, L. and Steven, G.P. A review on the modelling of piezoelectric sensors and actuators incorporated in intelligent structures, *J. Intell. Mater. Syst. Struct.*, 1998, **9**, (1), pp 3–19. <https://doi.org/10.1177/1045389X9800900101>
- [24] Preumont, A. Active structures for vibration suppression and precision pointing, *J. Struct. Contr.*, 1995, **2** (1), pp 49–63. <https://doi.org/10.1002/stc.4300020103>
- [25] Anonymous. *Abaqus Scripting User's Guide*. © Dassault Systèmes, 2022a.
- [26] Anonymous. *Abaqus User Subroutines Reference Guide*. © Dassault Systèmes, 2022b.
- [27] Virtanen, P., Gommers, R., et al. SciPy 1.0: Fundamental algorithms for scientific computing in python, *Nat. Methods*, 2020, **17**, pp 261–272. <https://doi.org/10.1038/s41592-019-0686-2>
- [28] Harris, C.R., Millman, K., et al. Array programming with NumPy. *Nature*, 2020, **585**, pp 357–362. <https://doi.org/10.1038/s41586-020-2649-2>
- [29] Boni, L., Bassetto, M., Quarta, A.A. and Mengali, G. Nonlinear dynamics of flexible heliogyro subject to sinusoidal root pitch command, *Aerosp. Sci. Technol.*, 2022, **130**, pp 1–9. Article no. 107920. <https://doi.org/10.1016/j.ast.2022.107920>

- [30] Boni, L., Bassetto, M., Niccolai, L., Mengali, G., Quarta, A.A., Circi, C., Pellegrini, R.C. and Cavallini, E. Structural response of helianthus solar sail during attitude maneuvers, *Aerosp. Sci. Technol.*, 2023, **133**, pp 1–9. Article no. 108152. <https://doi.org/10.1016/j.ast.2023.108152>
- [31] Fuller, S., Greiner, B., Moore, J., et al. The python control systems library (python-control), In *The 60th IEEE Conference on Decision and Control (CDC)*, 13–17 December, Austin, USA, 2021. IEEE Press. <https://doi.org/10.1109/CDC45484.2021.9683368>
- [32] Lew, J.-S., Juang, J.-N. and Longman, R.W. Comparison of several system identification methods for flexible structures, *J. Sound Vibr.*, **167** (3), pp 461–480, 1993. ISSN 0022-460X. <https://doi.org/10.1006/jsvi.1993.1348>
- [33] Juang, J.-N., Phan, M., Horta, L.G. and Longman, R.W. Identification of observer/Kalman filter Markov parameters-theory and experiments, *J. Guid. Contr. Dynam.*, 1993, **16**, (2), pp 320–329. <https://doi.org/10.2514/3.21006>
- [34] Phan, M., Horta, L.G., Juang, J.-N. and Longman, R.W. Linear system identification via an asymptotically stable observer, *J. Optim. Theory Appl.*, 1993, **79**, pp 59–86. <https://doi.org/10.1007/BF00941887>
- [35] Juang, J.-N. and Pappa, R.S. An eigensystem realization algorithm for modal parameter identification and model reduction, *J. Guid. Contr. Dynam.*, 1985, **8**, (5), pp 620–627. <https://doi.org/10.2514/3.20031>
- [36] Srinathkumar, S. Eigenvalue/eigenvector assignment using output feedback, *IEEE Trans. Automat. Contr.*, 1978, **23**, (1), pp 79–81. <https://doi.org/10.1109/TAC.1978.1101685>
- [37] Andry, A.N., Shapiro, E.Y. and Chung, J.C. Eigenstructure assignment for linear systems, *IEEE Trans. Aerosp. Electron. Syst.*, 1983, **AES-19**, (5), pp 711–729. <https://doi.org/10.1109/TAES.1983.309373>
- [38] Hilber, H.M. and Hughes, T.J.R. Collocation, dissipation and [overshoot] for time integration schemes in structural dynamics, *Earthquake Eng. Struct. Dynam.*, 1978, **6**, (1), pp 99–117. <https://doi.org/10.1002/eqe.4290060111>
- [39] Anonymous. *Abaqus Theory Manual*. © Dassault Systèmes, 2022c.